HHS Public Access

Author manuscript

Insect Biochem Mol Biol. Author manuscript; available in PMC 2021 October 01.

Published in final edited form as:

Insect Biochem Mol Biol. 2020 October ; 125: 103438. doi:10.1016/j.ibmb.2020.103438.

Iron binding and release properties of transferrin-1 from *Drosophila melanogaster* and *Manduca sexta*: implications for insect iron homeostasis

Jacob J. Weber[a], **Michael R. Kanost**[a], **Maureen J. Gorman**[a]

[a]Department of Biochemistry and Molecular Biophysics, Kansas State University, Manhattan, Kansas, 66506, U.S.A.

Abstract

Transferrins belong to an ancient family of extracellular proteins. The best-characterized transferrins are mammalian proteins that function in iron sequestration or iron transport; they accomplish these functions by having a high-affinity iron-binding site in each of their two homologous lobes. Insect hemolymph transferrins (Tsf1s) also function in iron sequestration and transport; however, sequence-based predictions of their iron-binding residues have suggested that most Tsf1s have a single, lower-affinity iron-binding site. To reconcile the apparent contradiction between the known physiological functions and predicted biochemical properties of Tsf1s, we purified and characterized the iron-binding properties of *Drosophila melanogaster* Tsf1 (DmTsf1), *Manduca sexta* Tsf1 (MsTsf1), and the amino-lobe of DmTsf1 ($DmTsf1_N$). Using UV-Vis spectroscopy, we found that these proteins bind iron, but they exhibit shifts in their spectra compared to mammalian transferrins. Through equilibrium dialysis experiments, we determined that DmTsf1 and MsTsf1 bind only one ferric ion; their affinity for iron is high (log K' = 18), but less than that of the well-characterized mammalian transferrins (log K' ~ 20); and they release iron under moderately acidic conditions (pH_{50} = 5.5). Iron release analysis of $DmTsf1_N$ suggested that iron binding in the amino-lobe is stabilized by the carboxyl-lobe. These findings will be critical for elucidating the mechanisms of Tsf1 function in iron sequestration and transport in insects.

Graphical Abstract

Corresponding author information: Maureen J. Gorman, Department of Biochemistry and Molecular Biophysics, 141 Chalmers, Kansas State University, Manhattan, KS 66506, U.S.A., mgorman@ksu.edu, 785-532-6922 .

Declarations of interest: none

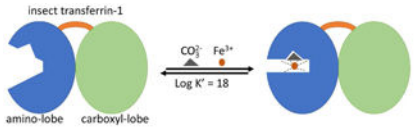

Protein	Putative Fe^{3+} coordinating residues	LMCT λ_{max} (nm)	Average Log K'	r_{max}	pH_{50}
MsTsf1	D Y Y Q	420	18.4	1.1	5.5
DmTsf1	E Y Y S	434	18.2	1.1	5.5
$DmTsf1_N$	E Y Y S	408	-	-	6.0

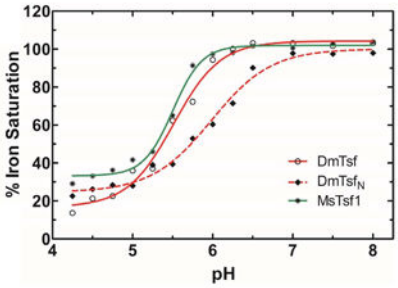

Keywords

transferrin; insect; iron binding; iron homeostasis; insect immunity; hemolymph

1. INTRODUCTION

Iron in animals is a double-edged sword: it is essential to critical cellular processes, yet dangerous due to potential interactions that create reactive oxygen species (Kosman, 2010). Iron is also an important factor in the immune system, as it is often the sought-after prize between a host and invading pathogens (Barber and Elde, 2015). Therefore, animals have a set of proteins that are involved in regulation, storage, transport, and sequestration of iron. Members of the transferrin superfamily are involved in carrying out a number of these functions (Baker, 1994). These secreted proteins are typically 70–80 kDa and structurally comprise two homologous lobes, an amino- and carboxyl-lobe, connected by a short linker sequence. Many have a high affinity ferric (Fe^{3+}) ion binding site in each lobe, thus, these proteins can protect cells by keeping free iron levels extremely low in extracellular environments (Aisen et al., 1978; Baldwin et al., 1984). The best-understood transferrins are those in mammals, including serum transferrin and lactoferrin. Serum transferrin binds and transports iron in the serum and delivers it into cells through a receptor-mediated endocytic pathway (Octave et al., 1983). Lactoferrin functions as an innate immune protein by sequestering iron in secreted fluids and blood (Farnaud and Evans, 2003; Jenssen and Hancock, 2009). A transferrin found in birds, ovotransferrin, has dual functions; it binds iron in the serum like serum transferrin and it sequesters iron in eggs like lactoferrin (Giansanti et al., 2012).

Crystal structures of serum transferrin, lactoferrin, and ovotransferrin have provided evidence for three common features of the Fe^{3+} binding sites: 1) four highly conserved amino acid ligands (an aspartate, a histidine and two tyrosines) whose side chains directly interact with the Fe^{3+} at the binding sites, 2) a synergistic anion cofactor, typically carbonate (CO_3^{2-}), and 3) two amino acid residues (threonine and arginine) that coordinate and hold the anion cofactor at the site (Anderson et al., 1989; Bailey et al., 1988; Kurokawa et al., 1995). A mutation of any of these six residues leads to accelerated release of iron, and mutations of the tyrosines can lead to a loss of iron binding (He et al., 1997b; Lambert et al., 2005; Mason and He, 2002; Mason et al., 2005; Ward et al., 1996).

The difference in physiological function between serum transferrin and lactoferrin is facilitated by a difference in iron binding ability at low pH. Serum transferrin binds to iron at neutral pH in serum, and, after it delivers iron into cells via endocytosis, the acidification of the endosome leads to release of iron over the pH range of 6.0 to 4.0 (Day et al., 1992). In contrast, lactoferrin retains iron unless the pH drops to 4.0 to 2.5 (Day et al., 1992). The difference in pH-mediated release comes from two factors: 1) in lactoferrin, cooperative interactions between the amino- and carboxyl-lobes help to stabilize the protein's iron binding sites, and 2) in serum transferrin, two lysine residues in the amino-lobe form a hydrogen-bond, but, upon acidification in the endosome, the lysines are protonated, leading to a charge repulsion that opens the lobe and releases the iron (Baker and Lindley, 1992; Day et al., 1992; Jameson et al., 1998; MacGillivray et al., 1998; Peterson et al., 2000; Ward et al., 1996).

Compared with the well-studied vertebrate transferrins, little is known about the biochemical properties of insect transferrins. The focus of this study is insect transferrin-1 (Tsf1). Similar to serum transferrin, Tsf1 is found in high concentrations in hemolymph; and, similar to lactoferrin, it is found in many secreted fluids (Bonilla et al., 2015; Brummett et al., 2017; Geiser and Winzerling, 2012; Hattori et al., 2015; Qu et al., 2014; Simmons et al., 2013; Zhang et al., 2014). Tsf1 appears to have a non-essential role in iron transport (Huebers et al., 1988; Kurama et al., 1995; Xiao et al., 2019), and it also protects insects from infection and oxidative stress by sequestering iron (Brummett et al., 2017; Geiser and Winzerling, 2012; Kim et al., 2008; Lee et al., 2006; Yoshiga et al., 1997). A puzzling aspect of Tsf1 comes from bioinformatic analyses. All Tsf1 amino-lobes have a predicted substitution, relative to the well-studied vertebrate transferrins, of at least one of the four iron-binding residues; moreover, carboxyl-lobe substitutions in many Tsf1 sequences indicate that those lobes do not bind iron (Geiser and Winzerling, 2012; Lambert et al., 2005). These observations suggest that most Tsf1s have a single lower-affinity iron binding site, but this prediction seems to be at odds with the known physiological functions of Tsf1s, which are all thought to involve high affinity iron binding.

Previous biochemical analyses of Tsf1 have not addressed this apparent contradiction between predicted biochemical properties and known biological functions. To date, biochemical analyses of Tsf1s have been limited to Tsf1 from the cockroach *Blaberus discoidalis* (BdTsf1) and Tsf1 from the moth *Manduca sexta* (MsTsf1). BdTsf1 has spectral and pH-mediated release properties that are similar to those of serum transferrin, but its affinity for iron is unknown (Gasdaska et al., 1996). It is not a very representative Tsf1 because, unlike most Tsf1s, it has residues for iron binding in both the amino- and carboxyl-lobes (Gasdaska et al., 1996; Lambert, 2012; Lambert et al., 2005). MsTsf1, which has a more representative sequence, also has spectral properties similar to those of the mammalian transferrins, but it binds only one ferric ion with unknown affinity (Bartfeld and Law, 1990; Huebers et al., 1988). No analyses of Tsf1 structure have been reported.

The goals of this study were to evaluate the iron binding and release properties of Tsf1s and to assess the functional role of a non-iron binding carboxyl-lobe. After evaluating the putative iron binding residues of 98 Tsf1 sequences, we decided to focus our biochemical studies on two representative Tsf1s: *Drosophila melanogaster* Tsf1 (DmTsf1) and MsTsf1.

By using spectroscopic characterization and equilibrium dialysis, we analyzed the iron binding and release properties of purified DmTsf1 and MsTsf1, and the amino-lobe of DmTsf1 ($DmTsf1_N$). We found that DmTsf1 and MsTsf1 have one metal binding site and a high affinity for Fe^{3+}, and that they released their iron in a pH-mediated manner that is comparable to serum transferrin's release of iron in the endosome. We also found that $DmTsf1_N$ coordinates and releases iron differently than the full-length DmTsf1, indicating that the carboxyl-lobe influences iron binding in the amino-lobe. This work furthers our understanding of the underlying mechanisms of iron homeostasis in insects.

2. MATERIALS AND METHODS

2.1. Sequence alignment for binding residue determination

Serum transferrin, lactoferrin, ovotransferrin and Tsf1 sequences were collected through the UniProt data base (UniProt Consortium, 2019). Redundant or partial sequences were removed. The orthology of the putative Tsf1 sequences was verified by phylogenetic analysis (not shown). A sequence alignment was created with Clustal Omega using the EMBL-EBI server (Madeira et al., 2019). Information (including order, species, and accession number) about each sequence used in the alignment is listed in Table S1.

2.2. Recombinant baculovirus production

A full length DmTsf1 cDNA (LP08340) was obtained from the Drosophila Genomics Resource Center. For full-length DmTsf1 expression, the cDNA was amplified by PCR with the use of forward (5'-GGATCCATGATGTCGCCGCAT-3') and reverse (5'-GCGGCCGCTCACT GCTTGGCAATC-3') primers, digested with *Bam*HI and *Not*I, and inserted into the pOET3 transfer plasmid. The flashBAC Gold system (Oxford Expression Technologies) was used to generate a recombinant baculovirus. For the $DmTsf1_N$ mutant, the amino-lobe amino acid sequence was predicted by analyzing alignments with structurally known transferrins using Clustal Omega at the EMBL-EBI server (Madeira et al., 2019). We used forward (5'-GTTGTTGGATCCATGAT GTCGCCGCAT-3') and reverse (5'-GAGCGTGATGGCAGTTGAGCGGCCGCGTTGTTT-3') primers to amplify the $DmTsf1_N$ cDNA, which encodes amino acid residues 1–379 followed by a stop codon, and then generated a recombinant baculovirus with the procedure we used for full-length DmTsf1.

2.3. Protein expression and purification

For DmTsf1 and $DmTsf1_N$, recombinant baculovirus was used to infect ~3 liters of Sf9 cells (at 2×10^6 cells/ml in Sf900III serum free medium) using an MOI of 1. After 48 h, cells were separated from the culture medium by centrifugation at 500 × *g*. Ammonium sulfate was added to the culture medium to 100% saturation, and protein precipitation was allowed to occur at 4°C for two days. The floating precipitate was collected with a pipet and dialyzed three times against 20 mM Tris, pH 8.3 (4°C). The dialyzed sample was applied to a Q-Sepharose Fast Flow column (1.5 × 10 cm), and proteins were eluted with a linear gradient of 0–1 M NaCl in 20 mM Tris, pH 8.4 (4°C). Fractions containing transferrin were pooled and concentrated with Amicon Ultracel centrifugal filters with a 30 kDa molecular weight cut-off and then applied to a HiLoad 16/60 Superdex 200 column (GE Healthcare)

equilibrated in 20 mM Tris, 150 mM NaCl, pH 7.4. $DmTsf1_N$ required an extra purification step. After the Superdex 200 column, fractions containing $DmTsf1_N$ were pooled and concentrated as described above. The sample was applied to an UnoQ column (Bio-Rad), and proteins were eluted using a linear gradient of 10–500 mM NaCl in 20 mM Tris, pH 8.3. Following this method, 35.0 mg of DmTsf1 was purified from 3.2 liters of infected cells, and 22.3 mg of $DmTsf1_N$ was purified from 3.0 liters of infected cells.

MsTsf1 was purified from hemolymph following a procedure previously described (Brummett et al., 2017) with minor modifications. Briefly, 96 larvae were reared to day two of the fifth instar larval stage. From the larvae, 120 mL of hemolymph was collected at 4°C into saturated ammonium sulfate and adjusted to a final saturation of 55%. The solution was stirred for 30 minutes to allow proteins to precipitate, followed by centrifugation at 12000 × *g* to remove precipitants. The remaining supernatant was dialyzed three times against 4 liters of 20 mM Tris, pH 8.3 (4°C). The sample was loaded onto a DEAE Sephacel column (2.5 × 22 cm), and proteins were eluted with a linear gradient of 0–120 mM NaCl in 20 mM Tris, pH 8.3 (4°C). Fractions were analyzed by western blot, pooled and concentrated with Amicon Ultracel centrifugal filters with a 30 kDa molecular weight cut-off. The concentrated sample was divided into two parts (~ 4 mL each), and each was applied to a HiLoad 16/60 Superdex 200 column (GE Healthcare) equilibrated in 20 mM Tris, 150 mM NaCl, pH 7.4. Fractions containing transferrin were pooled and concentrated, and the buffer was adjusted to 0.5 M NaCl. The sample was applied to a series of two 1 mL HiTrap ConA 4B columns (GE Healthcare), and bound proteins were eluted with buffer containing 20 mM Tris, 0.5 M NaCl, 1 mM $MnCl_2$, 1 mM $CaCl_2$, 0.5 M methyl-α-D-mannopyranoside, pH 7.4. Fractions containing transferrin were pooled, concentrated and dialyzed against 20 mM Tris, 10 mM NaCl, pH 8.3. The sample was applied to an UnoQ column (Bio-Rad), and proteins were eluted using a linear gradient of 10–500 mM NaCl in 20 mM Tris, pH 8.3. Following this method, 9.2 mg of MsTsf1 was purified from 120 mL of hemolymph.

2.4. Production of the apo- and holo-forms of MsTsf1, DmTsf1 and $DmTsf1_N$

It was previously reported that after purification of MsTsf1 the protein was already iron saturated (Brummett et al., 2017). To ensure this was true of the purified Tsf1s used for this study, an absorbance spectrum (from 250–700 nm) of each Tsf1 at ~ 5 mg/mL in 10 mM HEPES, 20 mM sodium bicarbonate, pH 7.4, was measured, then 0.1 molar equivalent of ferric-nitrilotriacetic acid was added and allowed to equilibrate for 5–10 minutes, and finally a spectrum was collected. We concluded that each Tsf1 sample was saturated after purification because their absorbance spectra (specifically the LMCT peak) did not change (data not shown).

The apo-form of the purified Tsf1s was made as previously described (Brummett et al., 2017) by dialyzing purified protein samples against two exchanges of 1 liter of 0.1 M sodium acetate, 10 mM EDTA, pH 5, and then removing the EDTA by dialysis against two exchanges of 1 liter of 10 mM HEPES, pH 7.4. The Tsf1 samples changed from a yellowish-orange color in their holo-form to colorless in their apo-form.

2.5. Equilibrium dialysis

Experimental conditions were adapted from previous studies on transferrins using equilibrium dialysis to measure Fe^{3+} affinity (Aisen et al., 1978; Tinoco et al., 2008). Measurements were made using microdialyzers composed of two cells separated by a 5 kDa molecular weight cut-off membrane (Nest Group Company). Apo-Tsf1s produced as described in section 2.4 were used. Dialysis buffer was composed of 1.5 mM citrate, 0.1 M sodium nitrate, 10 mM HEPES and 20 mM sodium bicarbonate, pH 7.4. Citrate keeps the Fe^{3+} from precipitating and does not compete with the carbonate anion at the binding site of the proteins (Aisen et al., 1978). Sodium nitrate was added to the dialysis buffer so that we could use previously calculated equilibrium constants for ferric-citrate complexes (Spiro et al., 1967; Warner and Weber, 1953). Known concentrations of either apo-DmTsf1 or apo-MsTsf1 in dialysis buffer were added to one cell of the dialyzer, while various concentrations of Fe^{3+}-citrate were added to both cells. Refer to Tables S2 and S3 for details on concentrations of apo-Tsf1 and Fe^{3+}-citrate used in each experiment and Figure S1 for a diagram of equilibrium dialysis experimental setup. Experiments were carried out at 25 ± 1°C, with gentle agitation over 2 days. Knowing the amount of apo-Tsf1, citrate and Fe^{3+} added allowed for the measurement of non-transferrin bound iron after dialysis via the FerroZine assay (see section 2.6) and the determination of the concentration Tsf1 bound iron, specific binding factor (r) and affinity constants.

2.6. Ferrozine-based assay

In order to measure the amount of non-transferrin bound iron after equilibrium dialysis, we used a Ferrozine-based assay (Stookey, 1970.). Ferrozine was added to $FeCl_3$ standards and samples, and the solutions were acidified and incubated at 25 ± 1°C with mild agitation for 18 hours to increase sensitivity (Jeitner, 2014). The amount of iron-Ferrozine complex was measured at 562 nm for each standard and sample. Standards were made in duplicates, and the resultant standard curve was used to determine the concentration of non-transferrin bound iron in solution from the equilibrium dialysis experiments.

2.7. Binding equations

Equations used for past studies of human transferrin's affinity for iron in a competitive environment with citrate (Aasa et al., 1963; Aisen et al., 1978) were modified to account for the single iron binding site of DmTsf1 and MsTsf1. Equation 1 (see below) is the overall reaction of free iron ($[Fe^{3+}]_{free}$), protein ([Tsf1]), the bicarbonate anion ($[HCO_3^-]$), their complex formation ($[Fe^{3+} \cdot Tsf1 \cdot CO_3^{2-}]$) along with the release of three protons at pH 7.4:

$$Fe^{3+} + Tsf1 + HCO_3^- \rightleftarrows \left(Fe^{3+} \cdot Tsf1 \cdot CO_3^{2-}\right) + 3H^+$$

$$K = \frac{\left[Fe^{3+} \cdot T_S f1 \cdot CO_3^{2-}\right]\left[H^+\right]^3}{\left[Fe^{3+}\right]_{free}[Tsf1][HCO_3^-]} \quad \text{(Equation 1)}$$

The complex $[Fe^{3+} \cdot Tsf1 \cdot CO_3^{2-}]$ in this situation is equal to the concentration of Tsf1 bound iron ($[Fe^{3+}]_{Tsf\ bound}$) calculated from an equilibrium dialysis experiment ($[Fe^{3+}]_{Tsf\ bound}$ values are found in Tables S2 and S3). Because Fe^{3+} in this situation is

chelated by citrate, the four known equilibrium equations for Fe^{3+}-citrate complexes were used to determine $[Fe^{3+}]_{free}$ (Spiro et al., 1967; Warner and Weber, 1953) and are as follows:

$$HCit(OH)^{2-} + Fe^{3+} \rightleftarrows FeCitO^{-} + 2H^{+}$$

$$K_{c1} = \frac{[Fecito^{-}]\left[H^{+}\right]^{2}}{\left[Fe^{3+}\right]\left[HCit(OH)^{2-}\right]} \quad \text{(Equation 2a)}$$

$$Cit(OH)^{3-} + Fe^{3+} \rightleftarrows FeCitO^{-} + H^{+}$$

$$K_{c2} = \frac{[Fecito^{-}]\left[H^{+}\right]}{\left[Fe^{3+}\right]\left[Cit(OH)^{3-}\right]} \quad \text{(Equation 2b)}$$

$$HCit(OH)^{2-} \rightleftarrows Cit(OH)^{3-} + H^{+}$$

$$K_{c3} = \frac{\left[Cit(OH)^{3-}\right]\left[H^{+}\right]}{\left[HCit(OH)^{2-}\right]} \quad \text{(Equation 2c)}$$

$$FeCitO^{-} + Cit(OH)^{3-} \rightleftarrows Fe(CitO)_{2}^{5-} + H^{+}$$

$$K_{c4} = \frac{\left[Fe(CitO)_{2}^{5-}\right]\left[H^{+}\right]}{[FeCitO^{-}]\left[Cit(OH)^{3-}\right]} \quad \text{(Equation 2d)}$$

Adhering to past procedures (Aisen et al., 1978), we used the following values for the Fe^{3+}-citrate equilibrium constants: log K_{c1} = 3.64; log K_{c2} = 9.46; log K_{c3} = −5.82; log K_{c4} = −6.17. Taken together with the known concentrations of citrate ($[Cit]_{add}$) and Fe^{3+} ($[Fe^{3+}]_{add}$) added to the equilibrium dialysis experiment, these equations provided us with enough information to determine citrate's effect on the concentration of $[Fe^{3+}]_{free}$ by Equation 3:

$$\left[Fe^{3+}\right]_{free} = \frac{(C_{eq})\left(\left(\left[H^{+}\right]^{2}\right)(K_{c2}) + \left(\left[H^{+}\right]\right)(K_{c1}) + (C_{eq})(K_{c1})(K_{c4})\right)}{(K_{c1})(K_{c2})\left([Cit]_{add} - \left[Fe^{3+}\right]_{add}\right)} \quad \text{(Equation 3)}$$

where $C_{eq} = \frac{-y + \left(y^{2} - 4xz\right)^{1/2}}{2x}$ and x = $(K_{c3})(K_{c4})$

$$y = \left(\left[H^{+}\right]\right)(K_{c3}) + \left[H^{+}\right]^{2} + ([Cit]_{add})(K_{c3})(K_{c4}) - (2)\left(\left[Fe^{3+}\right]_{add}\right)(K_{c3})(K_{c4})$$

$$z = -\left(\left(\left[Fe^{3+}\right]_{add}\right)\left(\left[H^{+}\right]\right)(K_{c3}) + \left(\left[Fe^{3+}\right]_{add}\right)\left(\left[H^{+}\right]^{2}\right)\right)$$

Because the reactions took place at a constant pH and [HCO_3^-], the overall affinity constant (K) can be corrected to give an effective affinity constant (K') using Equation 4 (Aasa et al., 1963; Aisen et al., 1978):

$$K' = \left(\frac{[HCO_3^-]}{[H^+]^3} \right) (K) \quad \text{(Equation 4)}$$

Using these equations and the equilibrium dialysis results in Tables S2 and S3, the average K' (M^{-1}) was calculated and is reported as log K' for DmTsf1 and MsTsf1. An example calculation using these equations can be found in Table S4.

2.8. Ultraviolet-visible spectroscopy

To characterize and analyze the LMCT λ_{max} caused by iron binding to serum transferrin, MsTsf1, DmTsf1 and $DmTsf1_N$, we followed previous procedures for generating difference spectra for transferrins complexed with metals (Gasdaska et al., 1996; Harris and Pecoraro, 1983). Apo-Tsf1s were prepared as described above in buffer containing 100 mM HEPES and 15 mM sodium bicarbonate at pH 7.4. Human apo-serum transferrin was purchased from Sigma and prepared in the same buffer. Apo-transferrin solutions at ~4 mg/mL were added to both a sample and reference well. Sufficient ferric-nitrilotriacetate was added to the sample to saturate iron binding, and an equal volume of buffer was added to the reference well. Nitrilotriacetate is both an Fe^{3+} chelator and can act as the synergistic anion bound to transferrins (Aisen et al., 1978). When it is bound to transferrin at the anion binding site, it can cause shifts in the LMCT λ_{max} compared to the carbonate, which is the typical anion in physiological conditions (He et al., 2000b). To avoid this artifact and to get a true comparison of LMCT peaks, the sodium bicarbonate concentration in the buffer was kept significantly higher than that of nitrilotriacetate. UV-Vis spectra from 280 to 900 nm were obtained, and saturation of the iron binding site was signified by no additional change in the LMCT λ_{max} after the addition of more iron. The difference spectrum for each transferrin was determined by subtracting the absorbance spectrum of the reference from the absorbance spectrum of the sample.

2.9. pH mediated iron release assay

Previous methods for iron release from transferrins as a function of pH were followed (Baker et al., 2003; Day et al., 1992; Nicholson et al., 1997). Human holo-lactoferrin was purchased from Sigma, and human holo-serum transferrin was made as described in section 2.8. The iron-saturated transferrin samples (~ 5 mg/mL) were extensively dialyzed for 24 to 48 hours against various buffers over the pH range of 2.0 to 8.0. The buffers used were as follows: 50 mM HEPES, 50 mM MES, 50 mM sodium acetate and 100 mM glycine-HCl. The Tsf1s were not dialyzed below a pH of 4 because they precipitated at low pH. The ratio of the absorbance of the LMCT λ_{max} for each sample before and after dialysis gave the percent saturation at each pH unit. The data were plotted and fit with a sigmoidal dose response curve using GraphPad Prism Software.

3. RESULTS

3.1. Conservation of iron binding residues in Tsf1s

Insect Tsf1s' iron binding residues have been previously predicted based on alignments with serum transferrins and lactoferrins (Baker, 1994; Geiser and Winzerling, 2012; Lambert et al., 2005). To enable us to choose representative Tsf1s for our study, we wanted a more comprehensive list of the substitutions in Tsf1s from many different orders of insects. By using a sequence alignment of 98 insect Tsf1s, two lactoferrins, two serum transferrins and two ovotransferrins, we were able to gather a comprehensive collection of the predicted residues involved in iron binding (Table 1). (Note that the numbering of iron-coordinating residues in Table 1 and in the rest of this paper are based on the position in the human serum transferrin sequence.)

Several consistencies in the alignments are worth describing. First, in the amino-lobe of Tsf1s, the iron-coordinating tyrosines (Tyr-95 and Tyr-188) are conserved in all 98 insects. Site-directed mutagenesis studies of these tyrosines in lactoferrin have shown that each is vital to the stability of the binding site (Ward et al., 1996). Also, in the Tsf1 amino-lobes, 97 out of the 98 sequences show conservation of the anion coordinating residues, Thr-120 and Arg-124. The anion and the residues that coordinate it are crucial to iron binding (Zak et al., 2002). Conservation of the two tyrosines and the two anion residues suggest that Tsf1s bind iron in their amino-lobe. Another consistent result is that none of the 98 Tsf1 amino-lobe sequences have the His-249. There are five different residues that are present in this position: Gln (68), Ser (13), Thr (12), Pro (5) and Met (1). (The number in parenthesis indicates the number of times it was found.) Previous studies have probed the importance of the His-249 residue in serum transferrin's and lactoferrin's iron binding and release properties (Grady et al., 1995; He et al., 2000a; He et al., 2000b; MacGillivray et al., 2000; Mason and He, 2002; Nicholson et al., 1997). All of the His-249 mutants could bind iron, but most of them more readily released iron in response to a decrease in pH.

Less consistently seen in the alignments is the substitution of Asp-63 with glutamate, which occurs in 30 of the 98 Tsf1 sequences. The D63E change, which extends this iron coordinating sidechain by one methyl group, has been studied by site-directed mutagenesis in the human serum transferrin amino-lobe (Baker et al., 2003; He et al., 1997a; He et al., 1997c). The D63E mutant had similar iron coordinating characteristics as the wild type amino-lobe, but it more readily released its iron in the presence of a chelator, and it released iron at a higher pH.

Only nine Tsf1s show conservation of iron-binding residues in their carboxyl-lobe. One of these, BdTsf1, has been analyzed biochemically and was found to bind two equivalents of iron and to release iron in a similar pH-mediated manner as serum transferrin (Gasdaska et al., 1996).

From the data provided in Table 1, we decided to study the binding properties of MsTsf1, because it would give insight into the effect of the common H249Q substitution, and DmTsf1 because it would provide insight into the combined effect of D63E and H249S substitutions.

3.2. Production of MsTsf1, DmTsf1, and DmTsf1$_N$

In order to analyze the biochemical properties of MsTsf1, DmTsf1, and DmTsf1$_N$, we needed to obtain pure forms of each protein. MsTsf1was purified from *M. sexta* larval hemolymph as previously described (Brummett et al., 2017) through a number of steps: ammonium sulfate precipitation, anion exchange chromatography, gel filtration and high resolution ion exchange chromatography. From 96 larvae, 120 ml of hemolymph was collected, and 9.2 mg of MsTsf1 (~ 67 kDa) was purified (Figure 1A). Recombinant full length DmTsf1 and DmTsf1$_N$ (residues 1–379) were expressed in an insect cell line using a baculovirus expression system. We used similar purification steps for these proteins: ammonium sulfate precipitation, anion exchange chromatography and gel filtration. DmTsf1$_N$ required an extra high resolution ion exchange chromatography step at the end of the process. From 3.2 liters of infected cells, 35.0 mg of DmTsf1 (~ 66 kDa) was purified, and from 3.0 liters of infected cells, 22.3 mg of DmTsf1$_N$ (~ 39.5 kDa) was purified (Figure 1A).

3.3. DmTsf1 and MsTsf1 spectroscopic characterization of the binding of Fe^{3+}

Holo-serum transferrin and holo-lactoferrin have a red-orange color that results from a ligand-to-metal charge transfer (LMCT) band caused by the excitation of a pi orbital electron, believed to be from the phenol group of one tyrosine ligand, into a dpi* orbital of the iron (Baker, 1994; Patch and Carrano, 1981). It was evident after purification of DmTsf1 and MsTsf1 that they bind iron, because the concentrated protein solutions had a yellow-orange color. After removal of the iron by dialysis in buffer at pH 5 in the presence of the iron chelator EDTA, the color of the apo-protein solutions was clear. This visible characteristic of holo-Tsf1 is similar to that of holo-serum transferrin and holo-lactoferrin but less red.

In diferric serum transferrin and lactoferrin, the LMCT band typically gives a pronounced λ_{max} of ~470 nm, but the peak can shift if the binding site is altered by substitution of the iron coordinating residues or a loss of one of the lobes (Day et al., 1992; He et al., 2000b; Nicholson et al., 1997; Peterson et al., 2000). The binding of metals at the site also perturbs pi-pi* transitions in the phenolic ring of the ligating tyrosines. This gives rise to characteristic absorption peaks in the UV region at ~295 and ~245 nm (Baker, 1994). The UV-Vis spectra for iron-bound DmTsf1 and MsTsf1 shows the characteristic absorption peaks in the UV region at ~295 nm (Figure S1). Thus, it is likely that the two iron coordinating tyrosine residues are conserved in the amino-lobe, as suggested by the alignment data in Table 1. However, the λ_{max} of the LMCT band in the visible region for both proteins is blue-shifted considerably from the 470 nm we observe for serum transferrin and lactoferrin (Figure 2). The λ_{max} is ~434 nm for DmTsf1 and ~420 nm for MsTsf1 (Table 2). We expected to see shifts in the LMCT bands because of the substitutions of D63E and H249S in DmTsf1 and H249Q in MsTsf1. These shifts of the LCMT band resemble those of His-249 and Asp-63 amino-lobe mutants of lactoferrin and serum transferrin, which exhibited blue-shifts in the range of 6 to 30 nm (He et al., 1997c; Nicholson et al., 1997). Like the alignment data, these results suggest that these Tsf1s coordinate iron binding differently than serum transferrin and lactoferrin.

In the case of $DmTsf1_N$, the λ_{max} was shifted even further, to ~408 nm, and is more of a shoulder of the large 295 nm peak. This result demonstrates that the amino-lobe can bind iron without the presence of the carboxyl-lobe. However, binding in $DmTsf1_N$ is different from that of the full-length DmTsf1, suggesting altered iron coordination and the possibility of decreased stability of iron binding—similar to other transferrin amino-lobe mutants (Day et al., 1992; Tinoco et al., 2008).

3.4. Fe^{3+} affinity of DmTsf1 and MsTsf1.

With the putative substitutions at the iron binding site in both DmTsf1 and MsTsf1, we questioned if these proteins have a strong affinity for Fe^{3+}. We also wanted to quantitatively test whether they bind only one Fe^{3+} ion. We employed an equilibrium dialysis technique to measure the affinity of DmTsf1 and MsTsf1 for Fe^{3+} in the presence of citrate and HCO_3^- at 25±1°C at pH 7.4. The specific binding (r) values derived from binding isotherms (Figure 3) show iron saturation of the Tsf1s occurring at an r_{max} of 1.11 for DmTsf1 and an r_{max} of 1.08 for MsTsf1 (Table 2). These results support the hypothesis, based on our alignment data, that many Tsf1s have only one Fe^{3+} binding site, and are consistent with the observation that iron makes up 0.05% of the weight of holo-MsTsf1 (Huebers, et al., 1988). These results, combined with the spectral evidence that $DmTsf1_N$ binds iron, demonstrate that binding occurs in the amino-lobe only. Moreover, these results quantitatively support our use of a single binding site model in determining affinity constants.

We used our equilibrium dialysis data (Tables S2 and S3) and binding equations (Materials and Methods section 2.7) to calculate the Fe^{3+} affinity of DmTsf1 and MsTsf1. The known binding constants of Fe^{3+}-citrate complexes (Equation 2a–c) (Spiro et al., 1967; Warner and Weber, 1953) were used to calculate the effective concentration of free Fe^{3+} in Equation 3. Under the assumption that three protons are being released from a single binding site upon binding of Fe^{3+} (Aisen et al., 1978; Tinoco et al., 2008), we calculated overall equilibrium constants (K) of the Fe^{3+}-Tsf1 complexes at pH 7.4 using Equation 1. Using Equation 4, the K values were then corrected for an environment with constant pH and HCO_3^- to get the effective dissociation constant (K') (an example calculation is provided in Table S4). The average log K' for DmTsf1 was 18.2, and the average log K' for MsTsf1 was 18.4. These values are less than those of human serum transferrin (amino-lobe log K' of 20.7 and carboxyl-lobe log K' of 19.4) under similar conditions (Aisen et al., 1978), although they indicate that both Tsf1s have a very high affinity for Fe^{3+} despite iron binding site substitutions.

3.5. pH-mediated iron release from DmTsf1, $DmTsf1_N$ and MsTsf1.

Iron retention as a function of pH is a major difference between lactoferrin and serum transferrin, and this difference is important to their function in either immunity, in the case of lactoferrin, or iron transport, in the case of serum transferrin (Baker, 1994; Day et al., 1992). A previous study demonstrated that BdTsf1 releases iron in a manner similar to that of serum transferrin in response to lowered pH (Gasdaska et al., 1996). We decided to examine the iron release profiles of the more representative DmTsf1 and MsTsf1 to provide more information about possible mechanisms of Tsf1 function in immunity and iron

transport. We also tested DmTsf1$_N$'s iron release properties, for insight into the possible role of the non-iron binding carboxyl-lobe in stabilizing iron coordination. Iron-saturated Tsf1 was dialyzed against buffers with a pH range of 2.0–8.0, and then percent iron-saturation was measured. Dialysis results indicate that both MsTsf1 and DmTsf1 behave similarly to serum transferrin, with an estimated pH_{50} of 5.5 for both proteins (Figure 4, Table 2). Nearly identical to the pH release profile of serum transferrin (Day et al., 1992), DmTsf1 starts to release its iron at pH 6.25, while MsTsf1 does not start release until pH 5.75. Interestingly, neither Tsf1 is as stable as serum transferrin or lactoferrin at a pH of less than 4, which causes DmTsf1 and MsTsf1 to precipitate. In contrast to the full length Tsf1, DmTsf1$_N$ begins to release iron at ~pH 7 and has a pH_{50} of 6.0, indicating that iron release in the amino-lobe is affected by the presence of the carboxyl-lobe.

4. DISCUSSION

4.1. Comparison of Tsf1s to serum transferrin and lactoferrin

We found that the LMCT peak for DmTsf1 and MsTsf1 is blue-shifted relative to serum transferrin and lactoferrin. This is consistent with mutation studies of the amino-lobe of human serum transferrin, where a D63E mutation showed a LMCT λ_{max} shift from 472 nm to 450 nm (He et al., 1997c). To our knowledge there have been no studies of the effects of a H249S substitution; however, studies of mutants with substitutions of His-249 with other polar and uncharged resides in the amino-lobe of lactoferrin showed a LMCT λ_{max} shift from 450 nm to 428 nm for H249Q and 426 nm for H249T (Nicholson et al., 1997). The spectral characteristics of DmTsf1 and MsTsf1 support the alignment data in suggesting that these two Tsf1s differ in some residues that coordinate iron compared with serum transferrin and lactoferrin.

The effective binding affinity (expressed as log *K*') of DmTsf1 and MsTsf1 for Fe^{3+} is lower than that of serum transferrin under similar conditions. Lower affinity is likely due to the predicted differences in iron coordinating residues. Although the Tsf1s have lower Fe^{3+} affinity than serum transferrin and lactoferrin, their affinity (log *K*' of 18) is extremely high and functionally comparable to those of serum transferrin and lactoferrin. It is likely that DmTsf1 and MsTsf1 have an affinity for iron that is suitable for a physiological role in iron scavenging—a similar assumption made for other transferrins with lower affinity (Tinoco et al., 2008).

Like serum transferrin and lactoferrin, Tsf1s release iron at lowered pH. Both DmTsf1 and MsTsf1 have a pH_{50} of 5.5. This value is somewhat surprising given the His-249 substitution in both Tsf1s. A mutation of this histidine in the amino-lobe of lactoferrin has a dramatic effect on pH stability, such that H253Q/G/P mutants release all iron at pH 7.1 or higher (Nicholson et al., 1997). Despite changes in their iron coordination, Tsf1s had profiles of pH mediated iron release that are nearly identical to that of serum transferrin. The fact that serum transferrin has an amino-lobe with a pH_{50} of 5.7 and a carboxyl-lobe with a pH_{50} of 4.7, enables it to release iron in the acidifying environment of the endosome (a property necessary for its role in iron transport) (Baker, 1994; Peterson et al., 2000). Localization of Tsf1 within endosomes has not been demonstrated, and a Tsf1-receptor has not been

identified in insects; however, the iron release properties of DmTsf1 and MsTsf1 support the possibility that Tsf1s could release iron in an endosomal environment.

4.2. Role of the DmTsf1 carboxyl-lobe

It appears that many Tsf1s have lost the ability to bind iron in their carboxyl-lobe. This conclusion is based on our finding that only nine out of 98 species have conserved iron-binding residues in their carboxyl-lobe, and also based on our demonstration that DmTsf1 and MsTsf1 have an r_{max} value of ~1, and, thus, must bind only one ferric ion. With these results in mind, we questioned the functional role of the carboxyl-lobe. One interesting hypothesis is that the carboxyl-lobe may act as a decoy for certain pathogens that have developed specific receptors to steal iron specifically from this lobe of transferrins (Yoshiga et al., 1997). Another possibility is that the carboxyl-lobe is needed for receptor recognition. When holo-serum transferrin is recognized by the transferrin receptor, there is a large surface interaction between the C1 domain of the carboxyl-lobe and the transferrin receptor (Cheng et al., 2004).

While the above hypotheses have yet to be tested, our results indicate that the carboxyl-lobe stabilizes iron binding in the amino-lobe of DmTsf1. $DmTsf1_N$, which lacks the entire carboxyl-lobe, has spectral characteristics that clearly show it is capable of binding iron; however, there is a blue-shift of the LMCT peak relative to the full-length DmTsf1. In addition, $DmTsf1_N$ released iron at a higher pH than full-length DmTsf1. (It is important to note that attempts to perform Fe^{3+} affinity experiments with $DmTsf1_N$ in a competitive environment with citrate failed. This failure is probably due to an inability of $DmTsf1_N$ to compete effectively with citrate for Fe^{3+}.) $DmTsf1_N$ had properties similar to an amino-lobe mutant of lactoferrin (Lf_N) but not an amino-lobe mutant of serum transferrin (sTf_N) (Day et al., 1992; Peterson et al., 2000). Lf_N has a noticeable blue-shift of its LMCT peak from 465 nm to 454 nm and an increase in its pH_{50} compared with full-length lactoferrin, whereas the sTf_N counterpart has a red-shift and no change in pH_{50}. The difference between Lf_N and sTf_N pH stability has been explained in part by inter-lobe interactions that occur in lactoferrin but not in serum transferrin. Therefore, we suggest a similar hypothesis for Tsf1s: the carboxyl-lobe has a functional role in stabilizing iron coordination and in mediating proper release of iron as a function of pH.

4.3. Implications for insect immunity and iron homeostasis

Previous physiological studies have shown that Tsf1 functions in immunity, iron transport, and the prevention of oxidative stress; however, the biochemical mechanisms underlying these physiological roles are still poorly understood (Brummett et al., 2017; Geiser and Winzerling, 2012; Huebers et al., 1988; Kim et al., 2008; Kurama et al., 1995; Lee et al., 2006; Xiao et al., 2019; Yoshiga et al., 1997). Our study provides important information for understanding these mechanisms.

Our results support the model that Tsf1 protects against infection by sequestering iron (Geiser and Winzerling, 2012; Brummett et al., 2017). We found that DmTsf1 and MsTsf1 bind iron with high affinity despite a difference in iron coordination properties compared with mammalian lactoferrin. In acidic conditions, the insect transferrins would not be as

efficient at withholding iron as lactoferrin; however, the ability of lactoferrin to withhold iron at low pH may have evolved specifically for secretion into mammalian milk, which ends up in the acidic digestive tract of infants (Baker, 1994).

Though there is no known Tsf1 receptor in insects, iron from Tsf1 can be transported into cells (Huebers et al., 1988). This observation and the high concentration of Tsf1 in the hemolymph suggest that Tsf1 has a role in iron transport. Our results demonstrating that Tsf1 has a high affinity for iron and the ability to release iron over a physiologically relevant pH range are particularly interesting regarding its proposed role in iron transport (Huebers et al., 1988; Xiao et al., 2019). Two recent models of how Tsf1 may function in iron transport include the following scenarios for iron-binding: 1) Tsf1 binds iron in the secretory pathway of the midgut cells and is secreted into the hemolymph as holo-Tsf1, and 2) apo-Tsf1 in the hemolymph binds to iron that has been exported out of the midgut cells by an unknown mechanism (Xiao et al., 2019). Our results are compatible with both proposed pathways. Although there is mild acidification of some compartments of the secretory pathway, including the Golgi complex (Schapiro and Grinstein, 2000), release of iron from Tsf1 does not occur until the pH drops below 6; therefore, Tsf1 could potentially be loaded with iron in the secretory system of midgut cells as the first model suggests. With high iron affinity of DmTsf1 and MsTsf1 at pH 7.4, apo-Tsf1 should bind iron in the hemolymph, as suggested by the second model. Future work is required to determine how holo-Tsf1 delivers iron into cells, but we have shown that Tsf1 would be capable of releasing iron in endosomes in a manner similar to that of serum transferrin.

Compared with the immune and iron transport functions of Tsf1, less is known about its ability to protect insects against oxidative stress. However, studies of two species of beetles have shown that Tsf1 is upregulated in response to various types of stress and that a lack of Tsf1 leads to increased oxidative stress (Kim et al., 2008; Lee et al., 2006). Our study supports the model that high concentrations of Tsf1 in hemolymph and other extracellular fluids would keep free iron levels exceedingly low and, thus, protect the insect from iron-induced oxidative stress.

Supplementary Material

Refer to Web version on PubMed Central for supplementary material.

ACKNOWLEDGEMENTS

We thank Michal Zolkiewski and Lawrence Davis for helpful suggestions regarding this work and Lisa Brummett for making the DmTsf1 recombinant baculovirus. This work was supported by National Science Foundation Grant 1656388 and National Institute of General Medical Sciences grant R37 GM041247. This is contribution 20–166-J from the Kansas Agricultural Experiment Station.

ABBREVIATIONS

BdTsf1	Tsf1 from *Blaberus discoidalis*
cDNA	complementary DNA
$CO32^{-}$	carbonate

DEAE	diethylaminoethyl
DmTsf1	Tsf1 from *Drosophila melanogaster*
DmTsf1$_N$	recombinant amino-lobe of DmTsf1
HCO_3^-	bicarbonate
Lf$_N$	lactoferrin amino-lobe mutant
LMCT	ligand-to-metal charge transfer
MOI	multiplicity of infection
MsTsf1	Tsf1 from *Manduca sexta*
pH$_{50}$	pH at 50% iron saturation
r	specific binding constant
Sf9	cell line from *Spodoptera frugiperda*
sTf$_N$	serum transferrin amino-lobe mutant
Tsf1	insect transferrin-1
UV-Vis	ultraviolet-visible

REFERENCES

Aasa R, Malmström BG, Saltman P, Vänngård T, 1963 The specific binding of iron(III) and copper(II) to transferrin and conalbumin. Biochim. Biophys. Acta 75, 203–222. 10.1016/0006-3002(63)90599-7 [PubMed: 14083902]

Aisen P, Leibman A, Zweier J, 1978 Stoichiometric and site characteristics of the binding of iron to human transferrin. J. Biol. Chem 253, 1930–1937. [PubMed: 204636]

Anderson BF, Baker HM, Dodson EJ, Norris GE, Rumball SV, Waters JM, Baker EN, 1987 Structure of human lactoferrin at 3.2-A resolution. Proc. Natl. Acad. Sci. U.S.A 84, 1769–1773. 10.1073/pnas.84.7.1769 [PubMed: 3470756]

Anderson BF, Baker HM, Norris GE, Rice DW, Baker EN, 1989 Structure of human lactoferrin: crystallographic structure analysis and refinement at 2.8 A resolution. J. Mol. Biol 209, 711–734. 10.1016/0022-2836(89)90602-5 [PubMed: 2585506]

Bai L, Qiao M, Zheng R, Deng C, Mei S, Chen W, 2016 Phylogenomic analysis of transferrin family from animals and plants. Comp. Biochem. Physiol. D 17, 1–8. 10.1016/j.cbd.2015.11.002

Bailey S, Evans RW, Garratt RC, Gorinsky B, Hasnain S, Horsburgh C, Jhoti H, Lindley PF, Mydin A, Sarra R, 1988 Molecular structure of serum transferrin at 3.3-A resolution. Biochemistry 27, 5804–5812. 10.1021/bi00415a061 [PubMed: 3179277]

Baker EN, 1994 Structure and reactivity of transferrins, in: Sykes AG (Ed.), Advances in Inorganic Chemistry. Academic Press, pp. 389–463. 10.1016/S0898-8838(08)60176-2

Baker EN, Lindley PF, 1992 New perspectives on the structure and function of transferrins. J. Inorg. Biochem 47, 147–160. 10.1016/0162-0134(92)84061-q [PubMed: 1431877]

Baker HM, He Q-Y, Briggs SK, Mason AB, Baker EN, 2003 Structural and functional consequences of binding site mutations in transferrin: crystal structures of the Asp63Glu and Arg124Ala mutants of the N-lobe of human transferrin. Biochemistry 42, 7084–7089. 10.1021/bi020689f [PubMed: 12795604]

Baldwin DA, Jenny ER, Aisen P, 1984 The effect of human serum transferrin and milk lactoferrin on hydroxyl radical formation from superoxide and hydrogen peroxide. J. Biol. Chem 259, 13391–13394. [PubMed: 6092375]

Barber MF, Elde NC, 2015 Buried treasure: evolutionary perspectives on microbial iron piracy. Trends Genet. 31, 627–636. 10.1016/j.tig.2015.09.001 [PubMed: 26431675]

Bartfeld NS, Law JH, 1990 Isolation and molecular cloning of transferrin from the tobacco hornworm, Manduca sexta. Sequence similarity to the vertebrate transferrins. J. Biol. Chem 265, 21684–21691. [PubMed: 2254322]

Bonilla ML, Todd C, Erlandson M, Andres J, 2015 Combining RNA-seq and proteomic profiling to identify seminal fluid proteins in the migratory grasshopper Melanoplus sanguinipes (F). BMC Genomics 16, 1096 10.1186/s12864-015-2327-1 [PubMed: 26694822]

Brummett LM, Kanost MR, Gorman MJ, 2017 The immune properties of Manduca sexta transferrin. Insect Biochem. Mol. Biol 81, 1–9. 10.1016/j.ibmb.2016.12.006 [PubMed: 27986638]

Calap-Quintana P, González-Fernández J, Sebastiá-Ortega N, Llorens JV, Moltó MD, 2017 Drosophila melanogaster models of metal-related human diseases and metal toxicity. Int. J. Mol. Sci 18 10.3390/ijms18071456

Cheng Y, Zak O, Aisen P, Harrison SC, Walz T, 2004 Structure of the human transferrin receptor-transferrin complex. Cell 116, 565–576. 10.1016/s0092-8674(04)00130-8 [PubMed: 14980223]

Day CL, Stowell KM, Baker EN, Tweedie JW, 1992 Studies of the N-terminal half of human lactoferrin produced from the cloned cDNA demonstrate that interlobe interactions modulate iron release. J. Biol. Chem 267, 13857–13862. [PubMed: 1378432]

Enns CA, Rutledge EA, Williams AM, 1996 The transferrin receptor, in: Lee AG (Ed.), Biomembranes: A Multi-Volume Treatise, Endoctosis and Exocytosis. JAI, pp. 255–287. 10.1016/S1874-5342(96)80012-2

Farnaud S, Evans RW, 2003 Lactoferrin - a multifunctional protein with antimicrobial properties. Mol. Immunol 40, 395–405. 10.1016/s0161-5890(03)00152-4 [PubMed: 14568385]

Gasdaska JR, Law JH, Bender CJ, Aisen P, 1996 Cockroach transferrin closely resembles vertebrate transferrins in its metal ion-binding properties: a spectroscopic study. J. Inorg. Biochem 64, 247–258. 10.1016/s0162-0134(96)00052-9 [PubMed: 8916413]

Geiser DL, Winzerling JJ, 2012 Insect transferrins: multifunctional proteins. Biochim. Biophys. Acta 1820, 437–451. 10.1016/j.bbagen.2011.07.011 [PubMed: 21810453]

Giansanti F, Leboffe L, Pitari G, Ippoliti R, Antonini G, 2012. Physiological roles of ovotransferrin. Biochim. Biophys. Acta 1820, 218–225. 10.1016/j.bbagen.2011.08.004 [PubMed: 21854833]

Grady JK, Mason AB, Woodworth RC, Chasteen ND, 1995 The effect of salt and site-directed mutations on the iron(III)-binding site of human serum transferrin as probed by EPR spectroscopy. Biochem. J 309, 403–410. 10.1042/bj3090403 [PubMed: 7626003]

Harris WR, Pecoraro VL, 1983 Thermodynamic binding constants for gallium transferrin. Biochemistry 22, 292–299. 10.1021/bi00271a010 [PubMed: 6402006]

Hattori M, Komatsu S, Noda H, Matsumoto Y, 2015 Proteome analysis of watery saliva secreted by green rice leafhopper, Nephotettix cincticeps. PloS One 10, e0123671 10.1371/journal.pone.0123671 [PubMed: 25909947]

He QY, Mason AB, Nguyen V, MacGillivray RT, Woodworth RC, 2000a The chloride effect is related to anion binding in determining the rate of iron release from the human transferrin N-lobe. Biochem. J 350, 909–915. [PubMed: 10970808]

He QY, Mason AB, Pakdaman R, Chasteen ND, Dixon BK, Tam BM, Nguyen V, MacGillivray RT, Woodworth RC, 2000b Mutations at the histidine 249 ligand profoundly alter the spectral and iron-binding properties of human serum transferrin N-lobe. Biochemistry 39, 1205–1210. 10.1021/bi9915216 [PubMed: 10684597]

He QY, Mason AB, Woodworth RC, 1997a Iron release from recombinant N-lobe and single point Asp63 mutants of human transferrin by EDTA. Biochem. J 328, 439–445. [PubMed: 9371699]

He QY, Mason AB, Woodworth RC, Tam BM, MacGillivray RT, Grady JK, Chasteen ND, 1997b Inequivalence of the two tyrosine ligands in the N-lobe of human serum transferrin. Biochemistry 36, 14853–14860. 10.1021/bi9719556 [PubMed: 9398207]

He QY, Mason AB, Woodworth RC, Tam BM, Wadsworth T, MacGillivray RT, 1997c Effects of mutations of aspartic acid 63 on the metal-binding properties of the recombinant N-lobe of human serum transferrin. Biochemistry 36, 5522–5528. 10.1021/bi963028p [PubMed: 9154935]

Huebers HA, Huebers E, Finch CA, Webb BA, Truman JW, Riddiford LM, Martin AW, Massover WH, 1988 Iron binding proteins and their roles in the tobacco hornworm, Manduca sexta (L.). J. Comp. Physiol. B 158, 291–300. 10.1007/bf00695327 [PubMed: 3192782]

Jameson GB, Anderson BF, Norris GE, Thomas DH, Baker EN, 1998 Structure of human apolactoferrin at 2.0 Å resolution. Refinement and analysis of ligand-induced conformational change. Acta Crystallogr. D 54, 1319–1335. 10.1107/S0907444998004417 [PubMed: 10089508]

Jeitner TM, 2014 Optimized ferrozine-based assay for dissolved iron. Anal. Biochem 454, 36–37. 10.1016/j.ab.2014.02.026 [PubMed: 24632099]

Jenssen H, Hancock REW, 2009 Antimicrobial properties of lactoferrin. Biochimie 91, 19–29. 10.1016/j.biochi.2008.05.015 [PubMed: 18573312]

Kim BY, Lee KS, Choo YM, Kim I, Je YH, Woo SD, Lee SM, Park HC, Sohn HD, Jin BR, 2008 Insect transferrin functions as an antioxidant protein in a beetle larva. Comp. Biochem. Physiol. B 150, 161–169. 10.1016/j.cbpb.2008.02.009 [PubMed: 18400534]

Kosman DJ, 2010 Redox cycling in iron uptake, efflux, and trafficking. J. Biol. Chem 285, 26729–26735. 10.1074/jbc.R110.113217 [PubMed: 20522542]

Kurama T, Kurata S, Natori S, 1995 Molecular characterization of an insect transferrin and its selective incorporation into eggs during oogenesis. Eur. J. Biochem 228, 229–235. 10.1111/j.1432-1033.1995.0229n.x [PubMed: 7705333]

Kurokawa H, Mikami B, Hirose M, 1995 Crystal structure of diferric hen ovotransferrin at 2.4 A resolution. J. Mol. Biol 254, 196–207. 10.1006/jmbi.1995.0611 [PubMed: 7490743]

Lambert LA, 2012 Molecular evolution of the transferrin family and associated receptors. Biochim. Biophys. Acta 1820, 244–255. 10.1016/j.bbagen.2011.06.002 [PubMed: 21693173]

Lambert LA, Perri H, Halbrooks PJ, Mason AB, 2005 Evolution of the transferrin family: conservation of residues associated with iron and anion binding. Comp. Biochem. Physiol. B 142, 129–141. 10.1016/j.cbpb.2005.07.007 [PubMed: 16111909]

Lee KS, Kim BY, Kim HJ, Seo SJ, Yoon HJ, Choi YS, Kim I, Han YS, Je YH, Lee SM, Kim DH, Sohn HD, Jin BR, 2006 Transferrin inhibits stress-induced apoptosis in a beetle. Free Radic. Biol. Med 41, 1151–1161. 10.1016/j.freeradbiomed.2006.07.001 [PubMed: 16962940]

MacGillivray RT, Bewley MC, Smith CA, He QY, Mason AB, Woodworth RC, Baker EN, 2000 Mutation of the iron ligand His 249 to Glu in the N-lobe of human transferrin abolishes the dilysine “trigger” but does not significantly affect iron release. Biochemistry 39, 1211–1216. 10.1021/bi991522y [PubMed: 10684598]

MacGillivray RT, Moore SA, Chen J, Anderson BF, Baker H, Luo Y, Bewley M, Smith CA, Murphy ME, Wang Y, Mason AB, Woodworth RC, Brayer GD, Baker EN, 1998 Two high-resolution crystal structures of the recombinant N-lobe of human transferrin reveal a structural change implicated in iron release. Biochemistry 37, 7919–7928. 10.1021/bi980355j [PubMed: 9609685]

Madeira F, Park YM, Lee J, Buso N, Gur T, Madhusoodanan N, Basutkar P, Tivey ARN, Potter SC, Finn RD, Lopez R, 2019 The EMBL-EBI search and sequence analysis tools APIs in 2019. Nucleic Acids Res. 47, W636–W641. 10.1093/nar/gkz268 [PubMed: 30976793]

Mandilaras K, Pathmanathan T, Missirlis F, 2013 Iron absorption in Drosophila melanogaster. Nutrients 5, 1622–1647. 10.3390/nu5051622 [PubMed: 23686013]

Mason A, He Q-Y, 2002 Molecular aspects of release of iron from transferrin. 10.1201/9780824744175.ch4

Mason AB, Halbrooks PJ, James NG, Connolly SA, Larouche JR, Smith VC, MacGillivray RTA, Chasteen ND, 2005 Mutational analysis of C-lobe ligands of human serum transferrin: Insights into the mechanism of iron release. Biochemistry 44, 8013–8021. 10.1021/bi050015f [PubMed: 15924420]

Nicholson H, Anderson BF, Bland T, Shewry SC, Tweedie JW, Baker EN, 1997 Mutagenesis of the histidine ligand in human lactoferrin: Iron binding properties and crystal structure of the histidine-253 → methionine mutant,. Biochemistry 36, 341–346. 10.1021/bi961908y [PubMed: 9003186]

Octave J-N, Schneider Y-J, Trouet A, Crichton RR, 1983 Iron uptake and utilization by mammalian cells. I: Cellular uptake of transferrin and iron. Trends Biochem. Sci 8, 217–220. 10.1016/0968-0004(83)90217-7

Patch MG, Carrano CJ, 1981 The origin of the visible absorption in metal transferrins. Inorg. Chim. Acta 56, L71–L73. 10.1016/S0020-1693(00)88536-9

Peterson NA, Anderson BF, Jameson GB, Tweedie JW, Baker EN, 2000 Crystal structure and iron-binding properties of the R210K mutant of the N-lobe of human lactoferrin: implications for iron release from transferrins. Biochemistry 39, 6625–6633. 10.1021/bi0001224 [PubMed: 10828980]

Qu M, Ma L, Chen P, Yang Q, 2014 Proteomic analysis of insect molting fluid with a focus on enzymes involved in chitin degradation. J. Proteome Res 13, 2931–2940. 10.1021/pr5000957 [PubMed: 24779478]

Schapiro FB, Grinstein S, 2000 Determinants of the pH of the Golgi complex. J. Biol. Chem 275, 21025–21032. 10.1074/jbc.M002386200 [PubMed: 10748071]

Simmons LW, Tan Y-F, Millar AH, 2013 Sperm and seminal fluid proteomes of the field cricket Teleogryllus oceanicus: identification of novel proteins transferred to females at mating. Insect Mol. Biol 22, 115–130. 10.1111/imb.12007 [PubMed: 23211034]

Spiro TG, Bates George, Saltman Paul, 1967 Hydrolytic polymerization of ferric citrate. II. Influence of excess citrate. J. Am. Chem. Soc 89, 5559–5562. 10.1021/ja00998a009

Stookey LL, 1970 Ferrozine - a new spectrophotometric reagent for iron. Anal. Chem 42, 779–781.

Tang X, Zhou B, 2013 Iron homeostasis in insects: Insights from Drosophila studies. IUBMB Life 65, 863–872. 10.1002/iub.1211 [PubMed: 24078394]

Tinoco AD, Peterson CW, Lucchese B, Doyle RP, Valentine AM, 2008 On the evolutionary significance and metal-binding characteristics of a monolobal transferrin from Ciona intestinalis. Proc. Natl. Acad. Sci. U.S.A 105, 3268–3273. 10.1073/pnas.0705037105 [PubMed: 18287008]

Consortium UniProt, 2019 UniProt: a worldwide hub of protein knowledge. Nucleic Acids Res. 47, D506–D515. 10.1093/nar/gky1049 [PubMed: 30395287]

Ward PP, Zhou X, Conneely OM, 1996 Cooperative interactions between the amino- and carboxyl-terminal lobes contribute to the unique iron-binding stability of lactoferrin. J. Biol. Chem 271, 12790–12794. 10.1074/jbc.271.22.12790 [PubMed: 8662718]

Warner RC, Weber I, 1953 The cupric and ferric citrate complexes. J. Am. Chem. Soc 75, 5086–5094. 10.1021/ja01116a055

Xiao G, Liu Z-H, Zhao M, Wang H-L, Zhou B, 2019 Transferrin 1 functions in iron trafficking and genetically interacts with ferritin in Drosophila melanogaster. Cell Rep. 26, 748–758.e5. 10.1016/j.celrep.2018.12.053 [PubMed: 30650364]

Yoshiga T, Hernandez VP, Fallon AM, Law JH, 1997 Mosquito transferrin, an acute-phase protein that is up-regulated upon infection. Proc. Natl. Acad. Sci. U.S.A 94, 12337–12342. 10.1073/pnas.94.23.12337 [PubMed: 9356450]

Zak O, Ikuta K, Aisen P, 2002 The synergistic anion-binding sites of human transferrin: chemical and physiological effects of site-directed mutagenesis. Biochemistry 41, 7416–7423. 10.1021/bi0160258 [PubMed: 12044175]

Zhang J, Lu A, Kong L, Zhang Q, Ling E, 2014 Functional analysis of insect molting fluid proteins on the protection and regulation of ecdysis. J. Biol. Chem 289, 35891–35906. 10.1074/jbc.M114.599597 [PubMed: 25368323]

Highlights

- *Manduca sexta* and *Drosophila melanogaster* transferrin 1 (Tsf1) bind one ferric ion
- These transferrins have a very high affinity for iron (log K' = 18)
- They release iron at the pH found in endosomes (pH_{50} = 5.5)
- Their iron binding and release properties support predicted biological functions

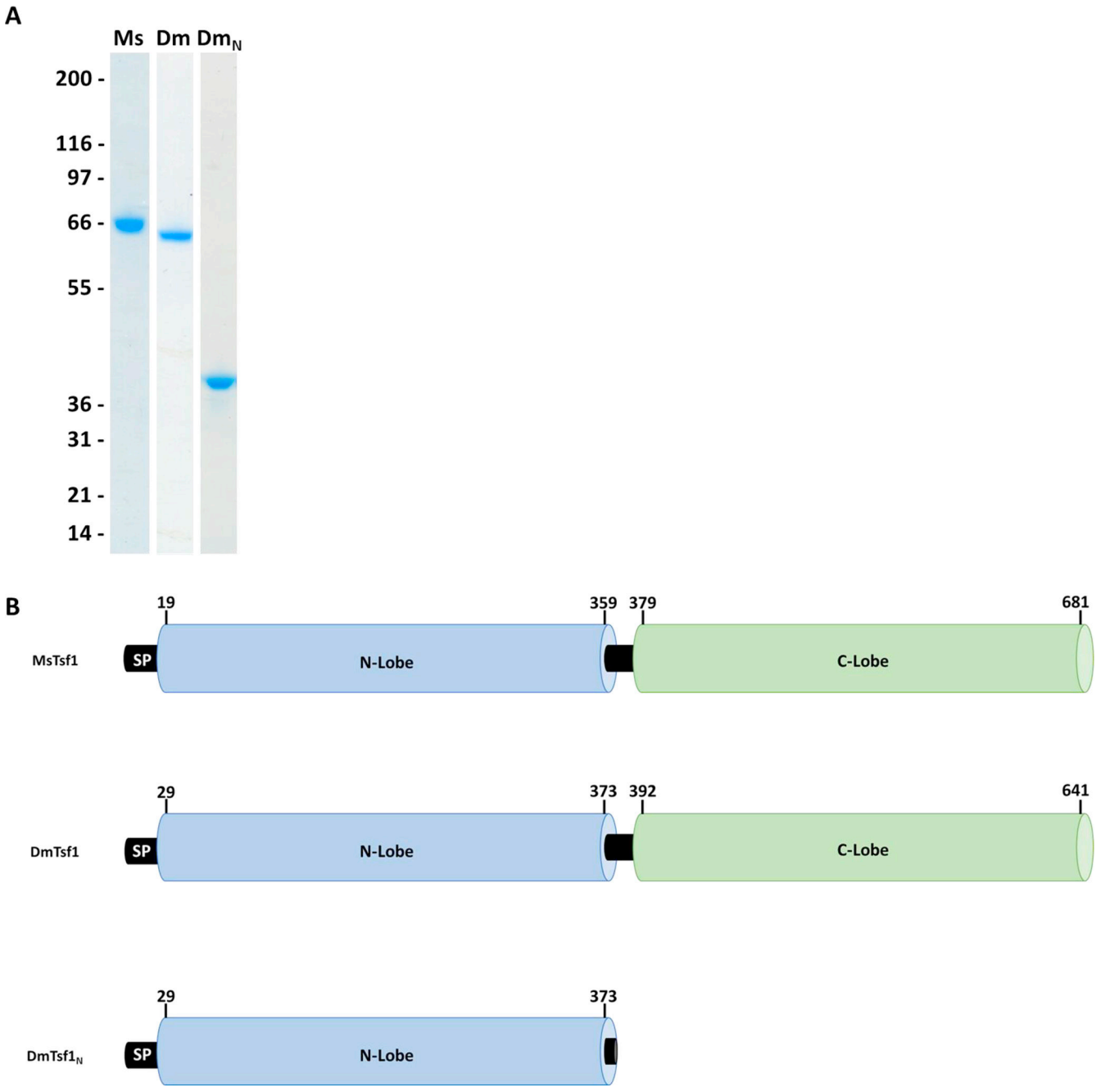

Figure 1. Analysis and domain architecture of purified Tsf1s.

(A) Tsf1 purified from the *M. sexta* larval hemolymph (Ms) and recombinantly expressed and purified *D. melanogaster* full-length (Dm) and amino-terminal lobe of Tsf1 (Dm_N) were analyzed by reducing SDS-PAGE followed by Coomassie staining. The positions of molecular mass standards are shown on the left and were used to estimate the size of the proteins. (B) The domain architecture of the purified Tsf1s based on alignment information. Represented here by their position in the amino acid sequence is the signal peptide (SP), the amino-lobe (N-lobe) colored in blue and carboxyl-lobe (C-lobe) in green.

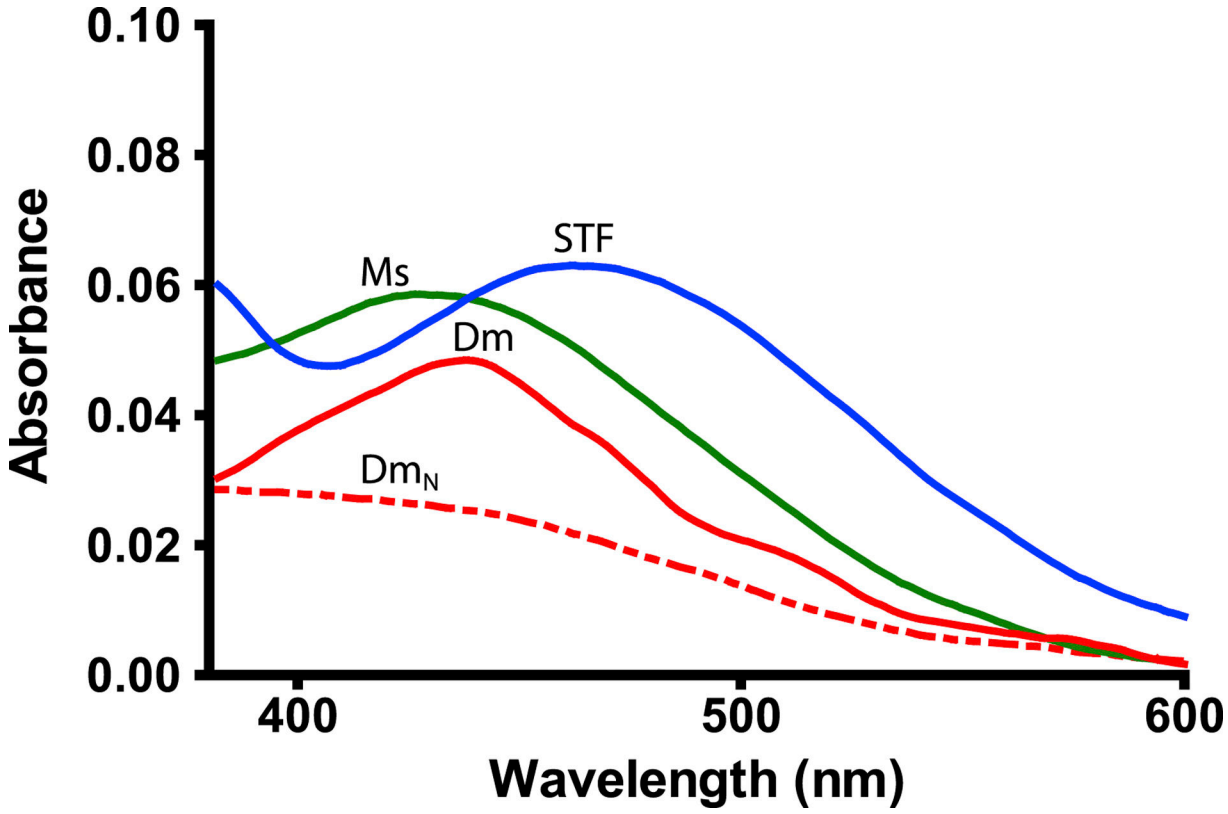

Figure 2. Visible difference spectra of the LMCT peak for the Fe^{3+}-transferrin complexes.
Serum transferrin (STF) is indicated by a blue line, MsTsf1 (Ms) by a green line, DmTsf1 (Dm) by a solid red line, and $DmTsf1_N$ (Dm_N) by a dashed red line. Proteins were at a concentration of approximately 4 mg/ml. The absorbance spectrum from the reference well containing the apo-protein was subtracted from the sample well containing fully iron-saturated holo-protein at the same concentration. A more complete spectrum showing the large 295 nm peak of each transferrin can be seen in Figure S1.

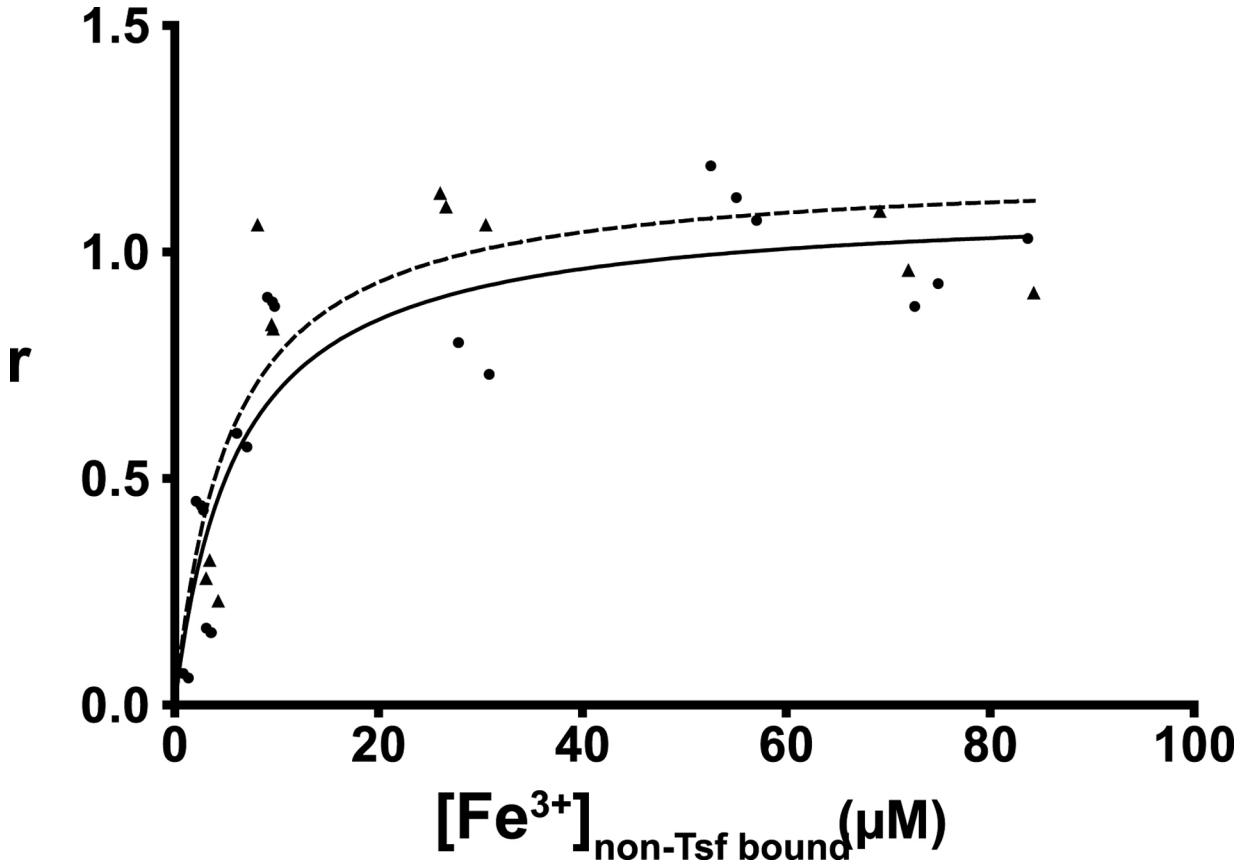

Figure 3. Binding isotherms of DmTsf1 and MsTsf1.

The DmTsf1 results are represented by dots and a solid line and MsTsf1 results by triangles and a dashed line. After equilibrium was reached in each experiment, the contents of the dialyzer were analyzed for the amount non-transferrin bound iron ($[Fe^{3+}]_{non\text{-}Tsf\ bound}$) using a ferrozine-based assay. From this assay the specific binding factor (r) for each experiment was determined by calculating the ratio of the concentration of transferrin bound iron ($[Fe^{3+}]_{Tsf\ bound}$) to the total Tsf1 concentration added [Tsf1] in the dialyzer. The r value at which saturation has occurred indicates the number of binding sites. Curve fitting and analysis of the r_{max} values (reported in Table 2) was performed using GraphPad Prism Software.

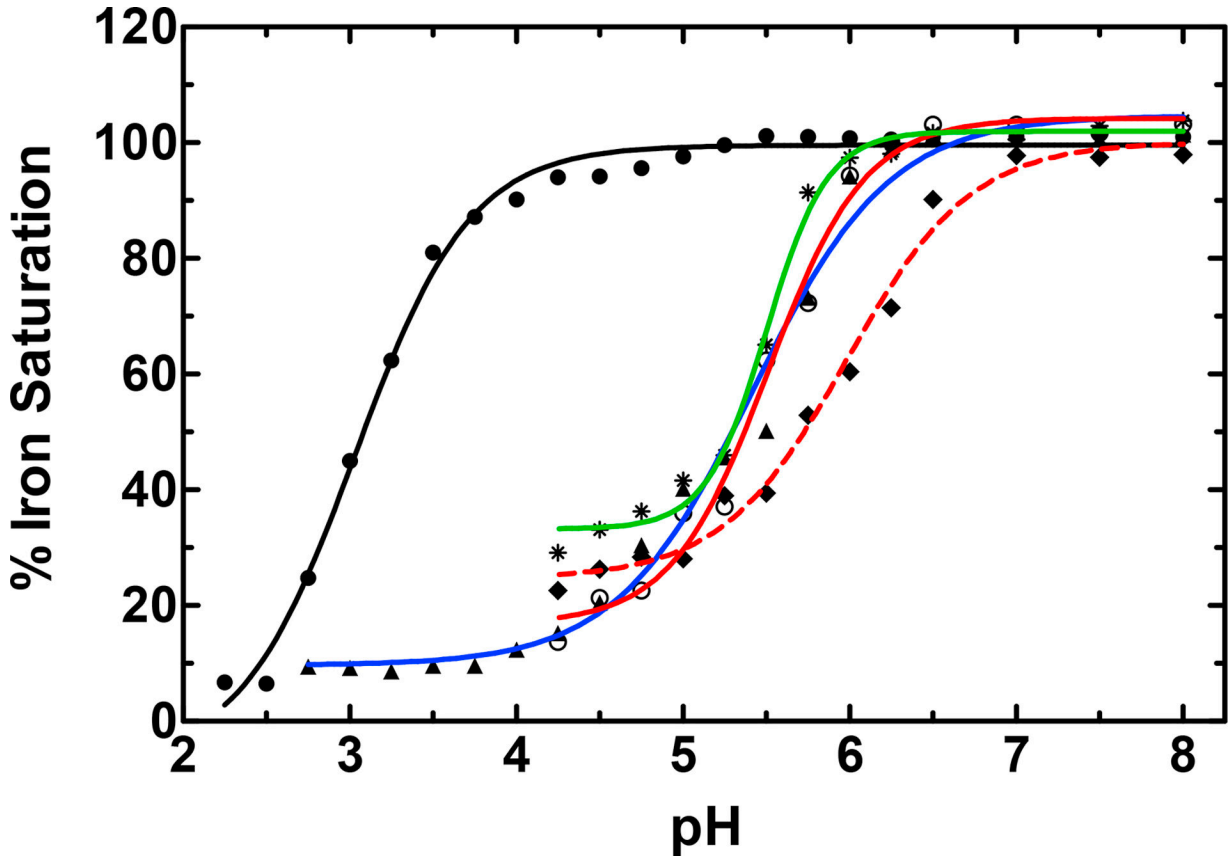

Figure 4. The pH-mediated release of iron from transferrins.

Serum transferrin is indicated by a blue line and triangles, lactoferrin by a black line and filled dots, MsTsf1 by a green line and asterisks, DmTsf1 by a solid red line and open dots, and $DmTsf1_N$ by a dashed red line and diamonds. Iron saturated protein samples, at ~5 mg/mL concentration, were dialyzed to equilibrium against various buffers at each indicated pH. The percent Fe^{3+}-saturation of the protein sample after dialysis was calculated by comparing the absorbance of the LMCT λ_{max} for each protein before and after dialysis. A sigmoidal dose response curve was used for curve fitting and analysis of the pH_{50} values (reported in Table 2).

Table 1.

Tsf1 residues predicted to be involved in iron and anion binding

	Amino-lobe						Carboxyl-lobe					
	Iron				Anion		Iron				Anion	
	D[a]	Y	Y	H	T	R	D	Y	Y	H	T	R
	63[b]	95	188	249	120	124	392	426	517	585	452	456
Blattodea												
(5[c])	+[d]	+	+	Q	+	+	+	+	+	+	+	+
Coleoptera												
(3)	+	+	+	Q	+	+	+	+	+	+	+	+
(2)	+	+	+	Q	+	+						
Diptera												
(21)	+	+	+	Q	+	+						
(13)	E	+	+	S	+	+						
(12)	E	+	+	T	+	+						
(1)	+	+	+	P	+	+						
(1)	E	+	+	M	+	+						
Hemiptera												
(5)	+	+	+	Q	+	+						
(4)	E	+	+	P	+	+						
Hymenoptera												
(16)	+	+	+	Q	+	+						
(1)	+	+	+	Q	+	L						
Lepidoptera												
(13)	+	+	+	Q	+	+						
Orthoptera												
(1)	+	+	+	Q	+	+	+	+	+	+	+	+

[a] Consensus iron and anion binding residues of serum transferrin, lactoferrin and ovotransferrin sequences are shown.

[b] Position numbers are based on human serum transferrin.

[c] The number in parentheses is the number of species within an order to have the particular sequence shown. Species and accession numbers are listed in Table S1.

[d] Plus signs indicate conservation of consensus residues; empty spaces indicate a lack of conservation.

Table 2.

Summary of the iron binding and release properties of MsTsf1, DmTsf1, $DmTsf1_N$, serum transferrin and lactoferrin

Protein	Fe^{3+} coordinating residues	LMCT λ_{max} (nm)	Average Log *K*	r_{max}	pH_{50} [c]
MsTsf1	D Y Y Q [a]	420	18.4	1.08	5.5
DmTsf1	E Y Y S [a]	434	18.2	1.11	5.5
$DmTsf1_N$	E Y Y S [a]	408	-	-	6.0
Serum transferrin amino-/carboxyl-lobe	D Y Y H	470	20.7 / 19.4 [b]	-	5.4
Lactoferrin	D Y Y H	470	-	-	3.0

[a] Putative residues determined through sequence alignments.

[b] Calculated from values of K_1' and K_2' from Aisen et al. (1978) (Aisen et al., 1978).

[c] pH at 50% iron saturation.